Luminosity Calorimeter

S. Denisov, S. Erin, N. Fedyakin, Yu. Gilitsky ,V.Sytnik
(IHEP, Protvino, Russia)

A precise measurement of the integrated the integrated luminosity will be required for the determination of the top mass from $\bar{t}t$ - cross section at threshold, as well as for the measurement of the W-boson couplings from W^+W^- - cross section [1]. In e^+e^- - colliders Bhabha scattering at small angles $e^+e^- \to e^+e^- (\gamma)$ is usually used to measure the luminosity. The dominance of the QED interaction in Bhabha scattering at small angles allows for the cross section to be calculated to a high precision and depends weekly on the properties of the Z^0 even close to the Z^0 pole.
To lowest order the small- angle Bhabha cross section is given by:

$$\sigma = \frac{16\pi\alpha^2}{s}\left(\frac{1}{\theta_{min}^2} - \frac{1}{\theta_{max}^2}\right)$$

where α-the fine structure constant , s- square of the center-of-mass energy, and θ - is a polar angle.
The process of calculating the luminosity involves triggering , identifying and classifying $e^+e^- \to e^+e^- (\gamma)$ events with high efficiency and small contamination from background sources.
Let us repeat the most important features of a detector for luminosity measurement [2]:

- Well-known geometry
- Very high and well-known trigger efficiency
- Small and well understood backgrounds
- Full coverage of the azimuthal angle

To achieve these goals the small angle gases calorimeter filled with heavy perfluoroalkane C_3F_8 with projective pad readout and micropattern tracker on GEM -base are proposed.
The essential features of this calorimeter are very high counting rate and radiation hard capability [3].
Extensive studies in gas ionization calorimeter have been performed in the last years [4-6].
The hadron/electromagnetic calorimeters with planar structure filled with gas mixture posses a number of attractive features like good energy resolution, high uniformity and stability, simple calibration and high intrinsic radiation hardness at low cost. The single disadvantage of this calorimeter is a high gas pressure necessary to obtain a reasonable signal/noise ratio.
We are proposed to use a heavy perfluoroalkane C_3F_8 as a working gas [4]. The choice of C_3F_8 is optimal for calorimeter applications for the following reasons:

- High density (4.4 times higher than that of a 90%Ar + 10%CF_4 mixture)
- High drift velocity
- Relatively low electron attachment rate

Prototype design.

The calorimeter tested consists of 32 longitudinal towers of ionization chambers with a flat geometry interleaved with 30-mm thick steel absorbers. Signal pads made of 1-mm steel were placed between absorbers forming two 3-mm gaps, which guarantees a full drift time $t_{dr} = 42$ ns at a given reduced field. There are 4 x 4 pads in the signal plane and the pad size is 76 x 76 mm^2. The total calorimeter thickness is more than $21X_0$. The absorbers were grounded and HV was applied to signal electrodes. The ratio of HV to pressure in case of C_3F_8 was about 830V/atm (v_{dr}~0.07mm/ns) [7], while tests with a mixture 90%Ar+10%CF_4 have been done with HV/P=185V/atm (v_{dr} ~ 0.12mm/ns) . The calorimeter was designed to operate at a pressure up to 16 atm.

To place the electronics away from the radiation hot area and to provide complete matching between preamplifier and tower, remote low –noise preamplifiers have been coupled to the corresponding front and back tower via cables of 4 m length with 25 Om impedance. This condition is extremely important if one wants to operate at very high counting rates.

Measurements and results.

All measurements of the calorimeter response and its resolution have been performed with 26.6 GeV/c e^- beam at the 70 GeV IHEP (Protvino) accelerator. The studies were carried out at different values of HV,ADC gate width and gas pressure. The events satisfying the following criteria were selected for the analysis:

- signals in any tower around the beam tower should be less than 10% of the signal in the beam tower;
- energy deposition in the front tower is higher than that in a back tower, while exceeding the noise level.

These criteria allow one to reject the events related to the muons, hadrons and beam halo. In the selected events more than 98% of the energy was released in 2 beam towers, while the signals in the neighboring towers have been essentially less than the noise level. That is why only beam tower signals have been used in the data analysis.

A typical distributions of noise and shower signal (P=5atm, t_g=59 ns) are presented in fig.2.

The dependence of the signal on the gas pressure are shown in fig.3 for the mixture 90%Ar+10%CF_4 (open circles) and for different C_3F_8 samples taken from the sources with different stated chemical purity (from 99% to 99.99%).

The fig.4 demonstrates that the signal responses, taken under different pressures, are not very sensitive to the HV. Quite good transversal uniformity can be illustrated by fig.5, where scan over transversal direction is shown.

It was proved that the energy resolution (after noise subtraction) does not depend on the C3F8 pressure (fig.6), which is consistent with our earlier

measurements, made with 90%Ar+10%CF_4 , and it scales with sample thickness as $\sqrt{t}$.

Future plans

We are going to perform Monte-Carlo simulation in order to optimize o the detector structure and geometry and to measure characteristies of the different absorbers(lead, tungsten),different absorber thickness and new electronics with improved signal-to-noise ratio. For better timing a plane of PPC will be used and/or a gap width will be reduced.

References:

[1.] Conceptual Design Report of a 500 Gev e^+e^- Linear Collider with Integrated X-ray Laser Facility DESY 1997-048,1997-182 Editors: R. Brikmann, G. Materlik,
J. Rossbach, A. Wagner

[2.] I.C.Brock et al., L3 Detector at LEP CERN-PPE/96-89

[3.] S.Denisov et al., Nucl. Instr. And Meth. A335 (1993) 106

[4.] S.Denisov et al., Nucl. Instr. And Meth. A 419 (1998) 590-595
A.Dushkin, et al. Instr. And Experiment. Techniques 5(1997) 12

[5.] D.Khazins et al., Nucl. Instr. And Meth. A 333(1993) 372

[6.] N.D. Giokaris et.al., Nucl. Instr. And Meth . A 333(1993) 364

[7.] S. Hunter et al., Phys. Rev. A 38 (1988) 58

Figure Captions

Fig. 1 The EMC module layout

Fig. 2 Noise and signal spectra (from electrons with E=26.6 GeV) measured at P= 5 atm of C_3F_8 and t_g= 59 ns

Fig.3 The average signal versus pressure for 90%Ar+10%CF_4 (opened symbols) mixture and freon C_3F_8(closed symboles)

Fig. 4 Signal variation with HV measured under different pressures of C_3F_8 and a mixture of 90%Ar+10%CF_4

Fig. 5 The transversal nonuniformity of the detector

Fig. 6 The dependence of the energy resolution on a C_3F_8 pressure (closed) and without (open) noise substraction

measurements, made with 90%Ar+10%CF_4 , and it scales with sample thickness as $\sqrt{t}$.

Future plans

We are going to perform Monte-Carlo simulation in order to optimize o the detector structure and geometry and to measure characteristies of the different absorbers(lead, tungsten),different absorber thickness and new electronics with improved signal-to-noise ratio. For better timing a plane of PPC will be used and/or a gap width will be reduced.

References:

[1.] Conceptual Design Report of a 500 Gev e^+e^- Linear Collider with Integrated X-ray Laser Facility DESY 1997-048,1997-182 Editors: R. Brikmann, G. Materlik,
J. Rossbach, A. Wagner

[2.] I.C.Brock et al., L3 Detector at LEP CERN-PPE/96-89

[3.] S.Denisov et al., Nucl. Instr. And Meth. A335 (1993) 106

[4.] S.Denisov et al., Nucl. Instr. And Meth. A 419 (1998) 590-595
A.Dushkin, et al. Instr. And Experiment. Techniques 5(1997) 12

[5.] D.Khazins et al., Nucl. Instr. And Meth. A 333(1993) 372

[6.] N.D. Giokaris et.al., Nucl. Instr. And Meth . A 333(1993) 364

[7.] S. Hunter et al., Phys. Rev. A 38 (1988) 58

Figure Captions

Fig. 1 The EMC module layout

Fig. 2 Noise and signal spectra (from electrons with E=26.6 GeV) measured at P= 5 atm of C_3F_8 and t_g= 59 ns

Fig.3 The average signal versus pressure for 90%Ar+10%CF_4 (opened symbols) mixture and freon C_3F_8(closed symboles)

Fig. 4 Signal variation with HV measured under different pressures of C_3F_8 and a mixture of 90%Ar+10%CF_4

Fig. 5 The transversal nonuniformity of the detector

Fig. 6 The dependence of the energy resolution on a C_3F_8 pressure (closed) and without (open) noise substraction

measurements, made with 90%Ar+10%CF_4 , and it scales with sample thickness as $\sqrt{t}$.

Future plans

We are going to perform Monte-Carlo simulation in order to optimize o the detector structure and geometry and to measure characteristies of the different absorbers(lead, tungsten),different absorber thickness and new electronics with improved signal-to-noise ratio. For better timing a plane of PPC will be used and/or a gap width will be reduced.

References:

[1.] Conceptual Design Report of a 500 Gev e^+e^- Linear Collider with Integrated X-ray Laser Facility DESY 1997-048,1997-182 Editors: R. Brikmann, G. Materlik,
J. Rossbach, A. Wagner
[2.] I.C.Brock et al., L3 Detector at LEP CERN-PPE/96-89
[3.] S.Denisov et al., Nucl. Instr. And Meth. A335 (1993) 106
[4.] S.Denisov et al., Nucl. Instr. And Meth. A 419 (1998) 590-595
A.Dushkin, et al. Instr. And Experiment. Techniques 5(1997) 12
[5.] D.Khazins et al., Nucl. Instr. And Meth. A 333(1993) 372
[6.] N.D. Giokaris et.al., Nucl. Instr. And Meth . A 333(1993) 364
[7.] S. Hunter et al., Phys. Rev. A 38 (1988) 58

Figure Captions

Fig. 1 The EMC module layout

Fig. 2 Noise and signal spectra (from electrons with E=26.6 GeV) measured at P= 5 atm of C_3F_8 and t_g= 59 ns

Fig.3 The average signal versus pressure for 90%Ar+10%CF_4 (opened symbols) mixture and freon C_3F_8(closed symboles)

Fig. 4 Signal variation with HV measured under different pressures of C_3F_8 and a mixture of 90%Ar+10%CF_4

Fig. 5 The transversal nonuniformity of the detector

Fig. 6 The dependence of the energy resolution on a C_3F_8 pressure (closed) and without (open) noise substraction

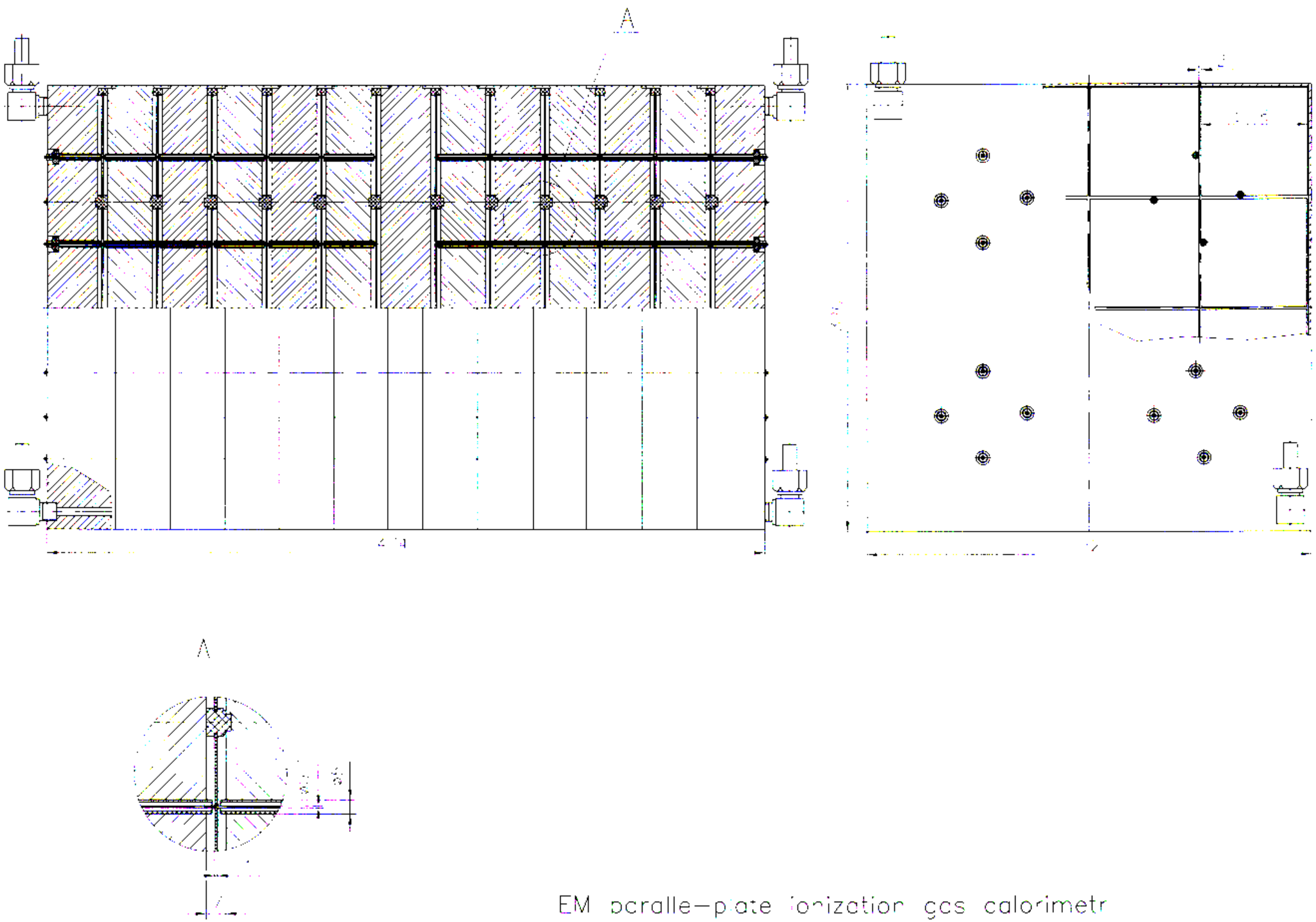

EM paralle-plate ionization gas calorimetr

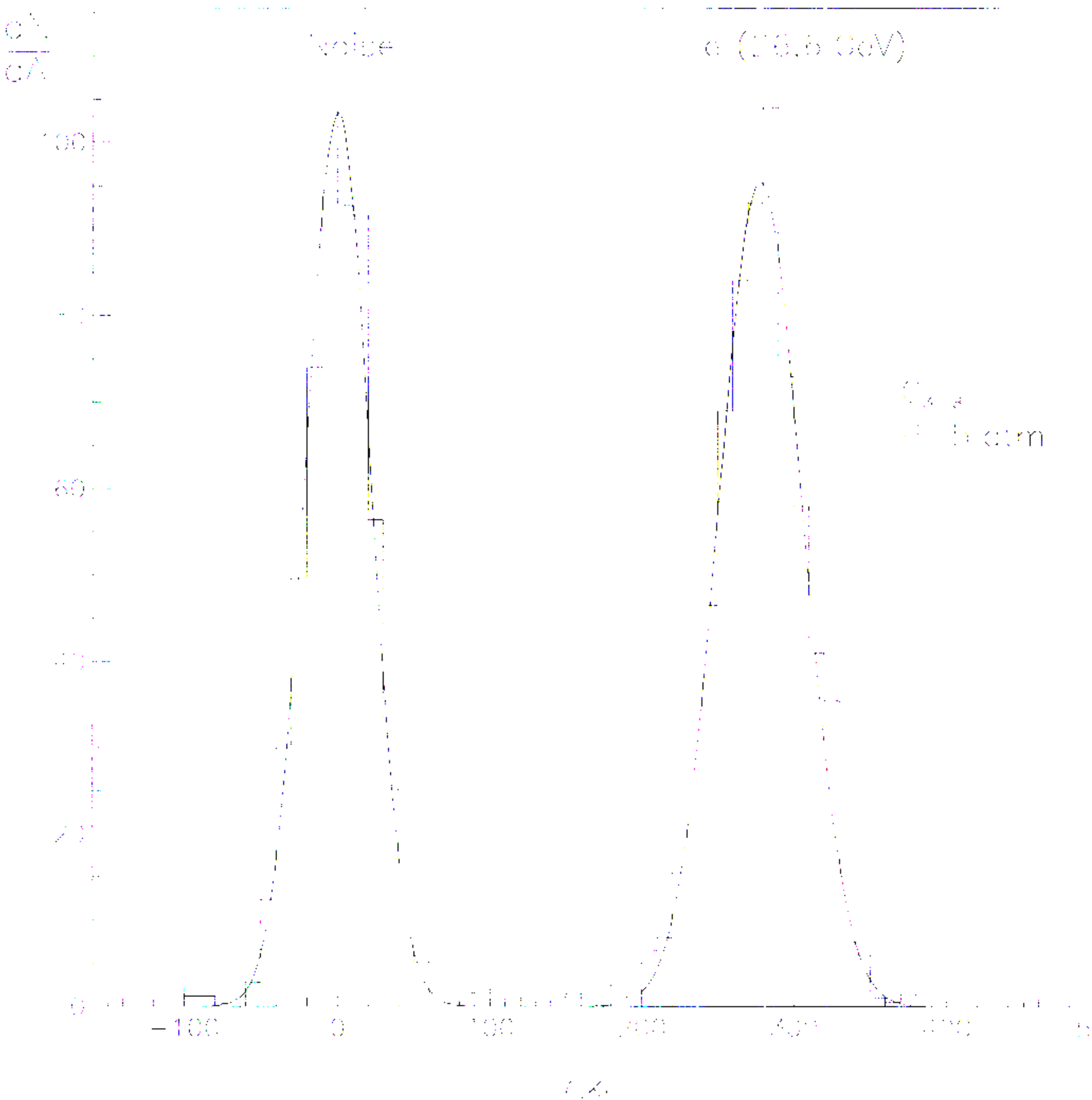

100
80
−100
0

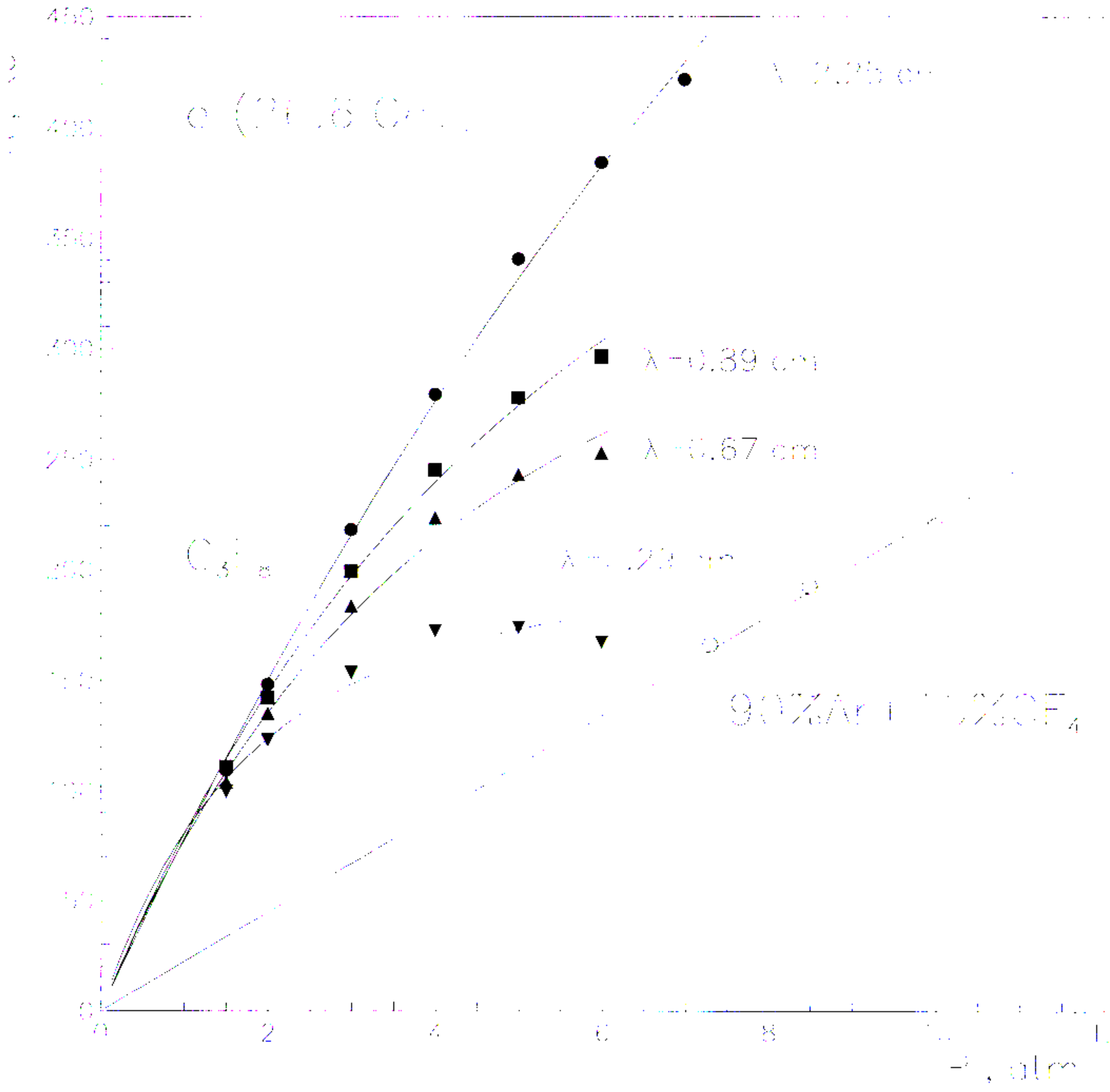

450
λ =0.39 cm
λ =0.67 cm
0
2
4
8

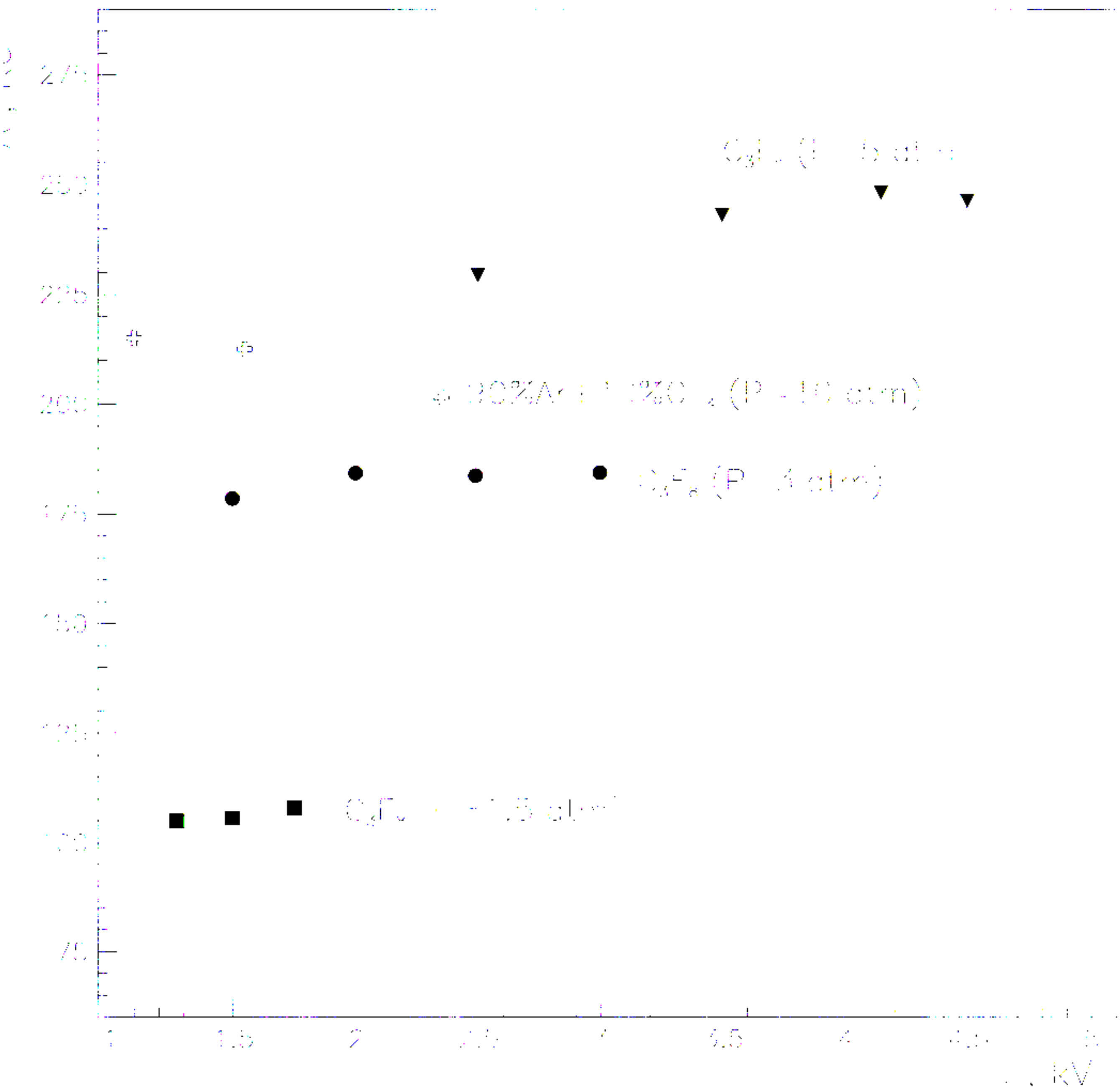

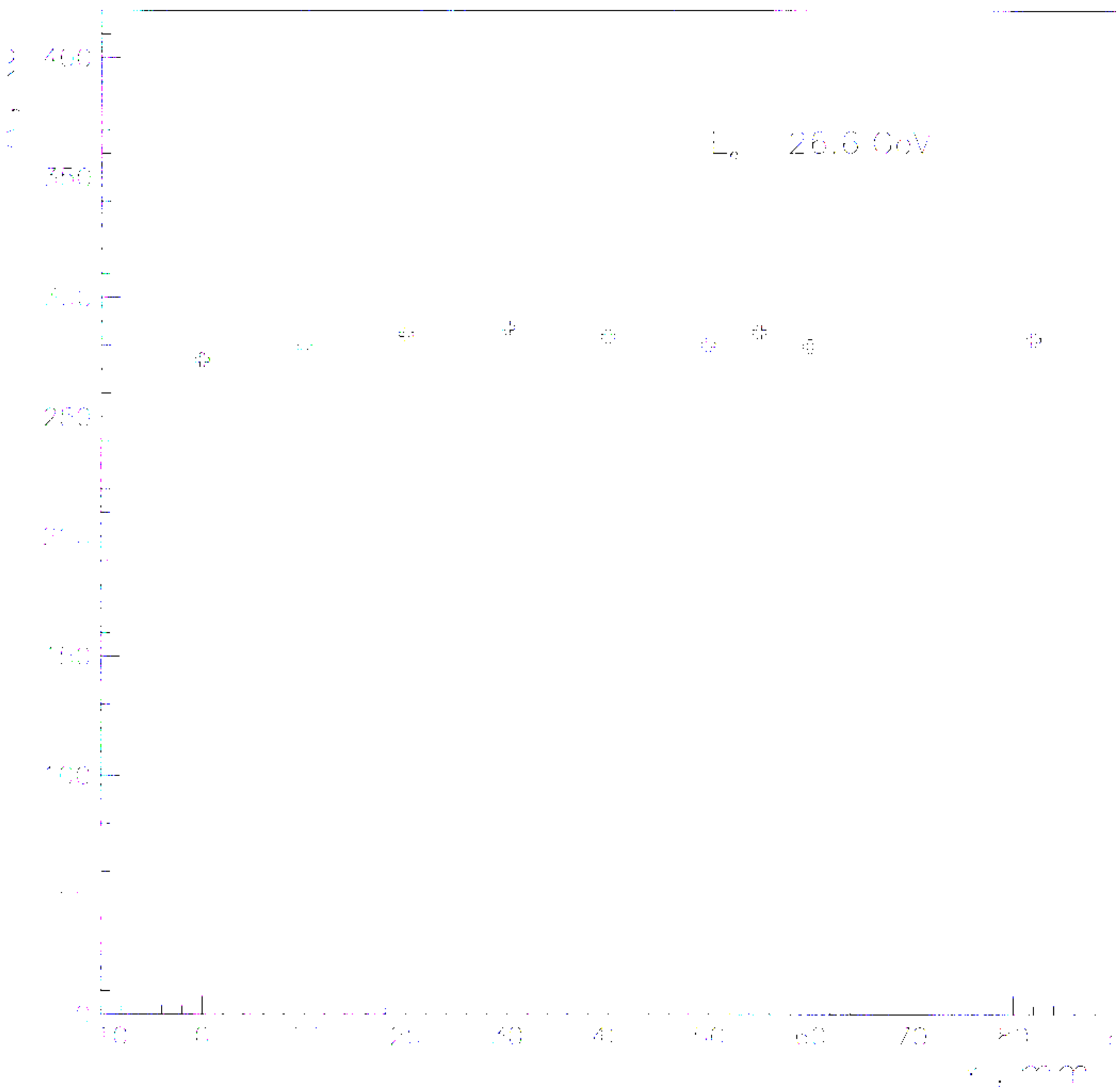
26.6 GeV

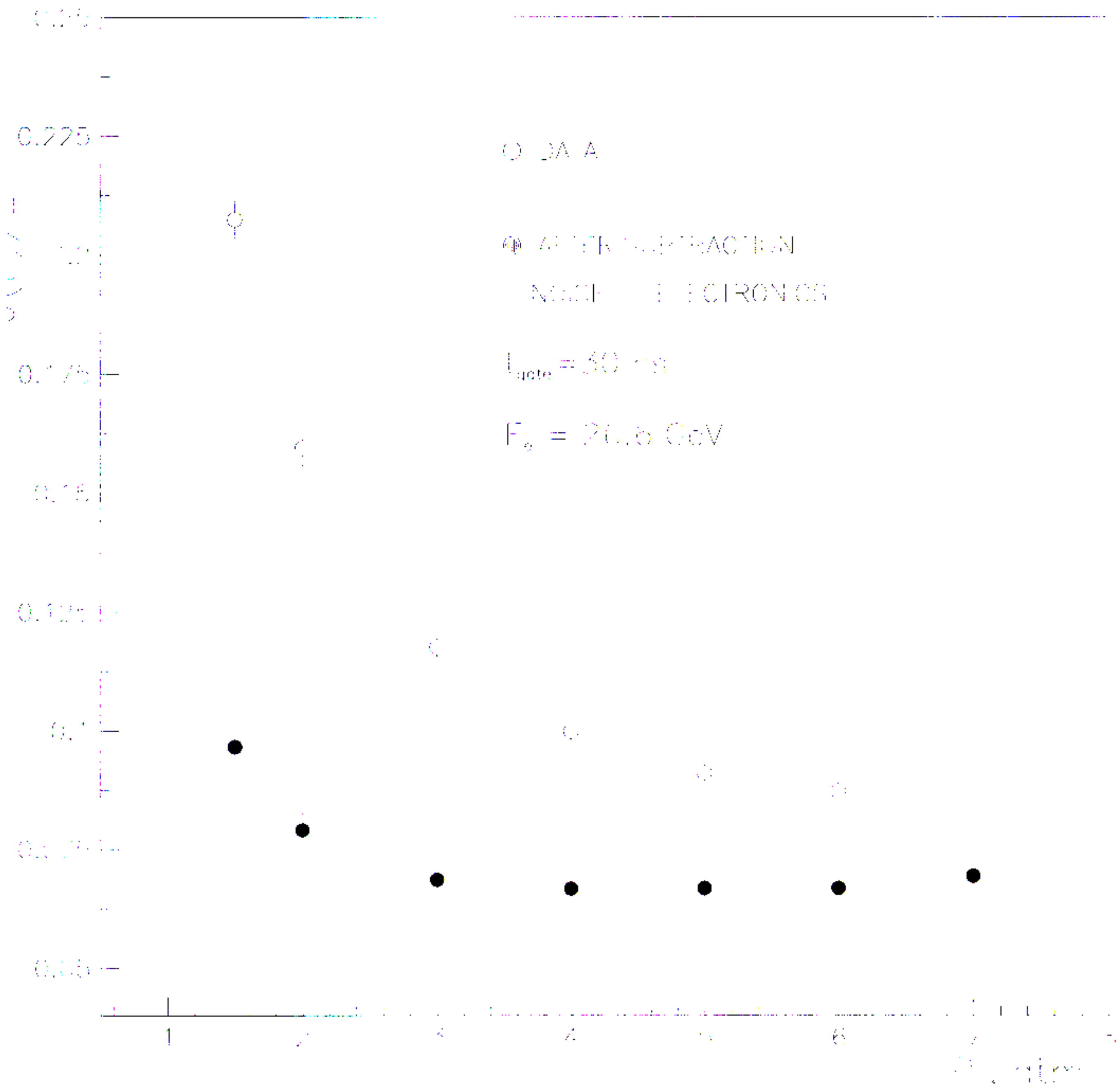
0.225
0.175
DATA
AFTER SUBTRACTION
ELECTRONICS
1
6